NEOPLASIA
www.neoplasia.com

Volume 20 Number 2 February 2018 pp. 131–139 131

Hypoxia Inducible Factors Modify Collagen I Fibers in MDA-MB-231 Triple Negative Breast Cancer Xenografts[1,2]

Eibhlin Goggins*,†, Samata Kakkad*, Yelena Mironchik*, Desmond Jacob*, Flonne Wildes*, Balaji Krishnamachary* and Zaver M. Bhujwalla*,‡

*Division of Cancer Imaging Research, The Russell H. Morgan Department of Radiology and Radiological Science, The Johns Hopkins University School of Medicine, Baltimore, MD, USA; †Department of Chemistry, Georgetown University, 37th and O Streets NW, Washington, D.C. 20057, USA; ‡Sidney Kimmel Comprehensive Cancer Center, The Johns Hopkins University, School of Medicine, Baltimore, MD, USA

Abstract

Hypoxia inducible factors (HIFs) are transcription factors that mediate the response of cells to hypoxia. HIFs have wide-ranging effects on metabolism, the tumor microenvironment (TME) and the extracellular matrix (ECM). Here we investigated the silencing effects of two of the three known isoforms, HIF-1α and HIF-2α, on collagen 1 (Col1) fibers, which form a major component of the ECM of tumors. Using a loss-of-function approach for HIF-1α or 2α or both HIF-1α and 2α, we identified a relationship between HIFs and Col1 fibers in MDA-MB-231 tumors. Tumors derived from MDA-MB-231 cells with HIF-1α or 2α or both HIF-1α and 2α silenced contained higher percent fiber volume and lower inter-fiber distance compared to tumors derived from empty vector MDA-MB-231 cells. Depending upon the type of silencing, we observed changes in Col1 degrading enzymes, and enzymes involved in Col1 synthesis and deposition. Additionally, a reduction in lysyl oxidase protein expression in HIF-down-regulated tumors suggests that more non-cross-linked fibers were present. Collectively these results identify the role of HIFs in modifying the ECM and the TME and provide new insights into the effects of hypoxia on the tumor ECM.

Neoplasia (2018) 20, 131–139

Introduction

Hypoxia and the stabilization of hypoxia inducible factors (HIFs) that mediate the adaptive response of cancer cells to hypoxia have been associated with increased invasiveness and metastasis [1]. Three known HIF isoforms, HIF-1α, HIF-2α and HIF-3α with separate as well as overlapping roles have been identified [2–4]. Of these, HIF-1α is the most widely investigated. Triple negative breast cancer (TNBC) is an aggressive form of breast cancer that occurs in 15–20% of breast cancer patients. TNBCs relapse, display refractory drug-resistance, and metastasize earlier than other subtypes [5,6]. In TNBCs, overexpression of HIF-1α was associated with poor outcome in early stage disease [7]. In a recent study, immunization against HIF-1α inhibited the growth of basal mammary tumors [8]. The same study showed elevation of HIF-1α-specific IgG in TNBC patients.

Abbreviations: Col1, Collagen I; DAB, 3,3′-diaminobenzedine; DS, Double Silenced; ECM, Extracellular Matrix; HIF, Hypoxia Inducible Factor; H&E, Hematoxylin and eosin; LOX, Lysyl Oxidase; MMP, Matrix Metalloproteinase; MT-MMP, Membrane-Type Matrix Metalloproteinase; P4H, Prolyl Hydroxylase; qRT-PCR, Quantitative Real Time Polymerase Chain Reaction; TME, Tumor Microenvironment; TNBC, Triple Negative Breast Cancer; SHG, Second Harmonic Generation; SMA, Smooth Muscle Actin.

Address all correspondence to: Zaver M. Bhujwalla, PhD, Division of Cancer Imaging Research, Department of Radiology and Radiological Science, The Johns Hopkins University School of Medicine, 720 Rutland Avenue, Rm 208C Traylor Building, Baltimore, MD 21205, USA. or Balaji Krishnamachary, PhD, Division of Cancer Imaging Research, Department of Radiology and Radiological Science, The Johns Hopkins University School of Medicine, 720 Rutland Avenue, Rm 217 Traylor Building, Baltimore, MD 21205, USA.
E-mail: zaver@mri.jhu.edu

[1] Support: NIH R01CA73850, R01CA82237, R35CA209960, and P30CA006973.
[2] Conflict of Interest: The authors have no potential conflicts of interest.
Received 21 September 2017; Revised 18 November 2017; Accepted 20 November 2017

1476-5586
https://doi.org/10.1016/j.neo.2017.11.010

Cancer cells invade and migrate through the ECM on their metastatic journey [9–11]. Hypoxia and HIFs can facilitate invasion and metastasis by regulation of degradative enzymes and remodeling of the ECM [12]. Collagen 1 (Col1) fibers are a major component of the tumor ECM [13]. Col1 fibers also play a role in tumor development and metastasis [13–15]. High Col1 fiber density has been associated with tumor aggressiveness [13–15]. In breast cancers, high Col1 fiber density has been associated with increased malignancy [14]. The COL1A1 and COL1A2 genes produce pro-α1(I) and pro-α2(I) chains of the type I procollagen [16]. Prolyl 4-hydroxylases (P4Hs) are enzymes that catalyze the hydroxylation of proline residues on the pre-pro-collagen chains to form 4-hydroxyproline [17]. The hydroxylation of proline is a crucial step in forming procollagen type I that eventually forms mature Col1 after cross-linking by lysyl oxidase (LOX) [18]. LOX and the LOX-like family are enzymes that catalyze the cross-linking of Col1 [19]. High LOX or LOX-like expression has been associated poor prognosis in breast cancer [20–23]. Additionally, LOX and LOX-L2 are up-regulated in highly metastatic breast cancer cells [24]. LOX expression was found to be induced by hypoxia and regulated by HIF-1 in triple negative breast cancer cells [25]. Recently, HIF response elements were identified in the human LOX gene promoter [26].

Matrix metalloproteinases (MMPs) are zinc-dependent endopeptidases that degrade ECM proteins. MMP-1 and MMP-14, specifically, degrade and remodel Col1 fibers [27]. MMP-1 has been found to promote tumor growth and metastasis particularly to the brain [28]. MMP-14, or MT1-MMP, is a member of the membrane-type MMP subfamily (MT-MMP). Whereas other MMPs are secreted, MT-MMPs are part of a subfamily expressed as active proteins on the surface of cells [29,30]. MT1-MMP has previously been linked to angiogenesis and invasion [31,32].

Here, for the first time, we investigated the relationship between down-regulation of HIF-1α, HIF-2α, or combined HIF-1α and HIF-2α, on Col1 fiber patterns detected with second harmonic generation (SHG) microscopy of MDA-MB-231 triple negative breast cancer xenografts. To identify the molecular mechanisms underlying the differences in Col1 fiber patterns, we assayed LOX, P4HA1, P4HA2, MMP-1 and MT1-MMP in these tumors. Since cancer associated fibroblasts (CAFs) are a major source of Col1 fibers in tumors, we determined the numbers of CAFs in these tumors [33,34]. Our data provide new insights into the role of HIFs in regulating the tumor ECM.

Materials and Methods

Cells and Cell Culture Conditions

Cloning and generation of MDA-MB-231 cells stably expressing shRNA against HIF-1α, HIF-2α and both HIF-1α and HIF-2α using lentiviral transduction were performed as previously described [35,36]. Cells were maintained in RPMI 1640 medium (Mediatech, Manassas, VA, USA) supplemented with 10% fetal bovine serum (Sigma, St. Louis, MO), and maintained at 37 °C in a CO_2 incubator.

Tumor Studies

MDA-MB-231 cells expressing shRNA against HIF-1α (231-1α), HIF2-α (231-2α), or double silenced (231-DS) with cells expressing shRNA against both HIF-1α and HIF2-α were established using lentiviral transduction as previously described [35,36]. Engineered cells (2×10^6) were orthotopically inoculated in the mammary fat pad of female SCID mice, and monitored for tumor growth. Tumors were excised (231-EV, n = 10; 231-1α, n = 9; 231-2α, n = 8; 231-DS, n = 7) and used for *ex vivo* imaging and molecular analysis once tumor volumes were ~300 to 450 mm^3. All animal handling was conducted in accordance with the regulations outlined by the Institutional Animal Care and Use Committee of Johns Hopkins University.

SHG Microscopy

Briefly, tumors were paraffin-embedded and 5 μm thick sections obtained for immunohistochemical analysis. Hematoxylin and eosin (H&E) stained tumor sections were analyzed with SHG microscopy using an Olympus Laser Scanning FV1000 MPE multiphoton microscope (Olympus Corp., Center Valley, PA, USA) with a 25Xw/1.05XLPLN MP lens. Excitation was achieved at 860 nm and the second harmonic signal was detected at a wavelength of 430 nm. Multiple fields of view (FOVs) were acquired from each tumor section with a FOV of 423.52 × 423.52 μm^2. FOVs were spaced randomly throughout the tumor slide, avoiding necrotic regions. At least 6 FOVs were analyzed per tumor.

Quantification of fiber parameters including percent fiber volume and inter-fiber distance was performed using an in-house fiber analysis software as previously described [37]. The software was written using MATLAB 7.4.0 (The MathWorks, Natick, MA, USA).

RNA Isolation and qRT-PCR

RNA was isolated following a standard protocol (Qiagen, Valencia, CA, USA), and cDNA was synthesized using an iScript cDNA synthesis kit (Bio-Rad, Hercules, CA, USA). Briefly, tissue was homogenized with RLT buffer and passed through a QIAshredder to obtain RNA.

Quantitative real-time PCR (qRT-PCR) was performed using IQ SYBR Green Supermix and gene specific primers in the iCycler RT-PCR detection system (Bio-Rad, Hercules, CA, USA); 1 μl of 1:10 diluted cDNA was used. The expression of each gene was calculated relative to the house keeping gene, hypoxanthine phosphoribosyltransferase-1 (HPRT-1). The fold change between 231-HIF silenced and 231-EV tumors was calculated by comparing the change in threshold cycle (ΔCT) values. Confidence intervals were calculated based on a previously described model [38].

Protein Isolation and Immunoblotting

Protein expression levels of COL1A1, MMP-1, MMP-14, and LOX were quantified by immunoblotting. Approximately 100 μg of the whole cell protein lysates from tumor tissue, along with a prestained, broad range standard molecular weight marker were resolved on a 7% polyacrylamide gel. Proteins were transferred to a nitrocellulose membrane overnight after which the membrane was removed, blocked with 5% nonfat milk for 2 h and further incubated overnight with antibody. Antibodies used were rabbit-polyclonal anti-COL1A1 antibody (1:1000; OriGene, Rockville, MD, USA), rabbit polyclonal anti-MMP-1 antibody (1:1000 dilution; Neo BioLab, Woburn, MA, USA), rabbit polyclonal anti-MMP-14 antibody (1:1000 dilution; Neo BioLab, Woburn, MA, USA), mouse monoclonal anti-LOX antibody (1:1000 dilution; GeneTex, Inc., Irvine, CA, USA), or rabbit polyclonal anti-LOX-L1 antibody (1:1000 dilution; Sigma-Aldrich Corp. St. Louis, MO, USA). Horseradish peroxidase-conjugated secondary antibodies were used

at 1:2000 dilution. Blots were visualized using the SuperSignal West Pico Chemiluminescent substrate kit (Thermo Scientific, Rockford, IL, USA). The reference band from the molecular weight marker was used to determine the location of the protein of interest.

Immunohistochemistry Analysis

Formalin-fixed slides were stained for alpha smooth muscle actin (α-SMA), COL1A1, HIF-1α, and HIF-2α. For α-SMA, antigen retrieval was performed by boiling the sample in citrate buffer pH 6 in a microwave for 12 minutes. Slides were stained for α-SMA using a mouse-monoclonal anti-α-SMA antibody with a dilution of 1:200 (Novus Biologicals, Littleton, CO, USA). Slides were incubated overnight at 4 °C. Following this, sections were incubated with horseradish peroxidase conjugated with anti-mouse IgG. Slides were then stained with 3,3′-diaminobenzedine (DAB) and counterstained with hematoxylin.

For COL1A1 immunostaining, antigen retrieval was performed in citrate buffer pH 6 in the microwave for 15 minutes after which slides were stained using rabbit-polyclonal anti-COL1A1 antibody (OriGene, Rockville, MD, USA) at a dilution of 1:70. After overnight incubation at 4 °C, sections were incubated with horseradish peroxidase conjugated with anti-rabbit IgG. Slides were again stained with DAB and counterstained with hematoxylin.

For HIF-1α and HIF-2α immunostaining, slides were placed in a steamer with citrate buffer pH 6 for 50 and 30 minutes, respectively, for antigen retrieval. Mouse monoclonal HIF-1α primary antibody with a dilution of 1:8000 (Novus Biologicals, Littleton, CO, USA) or HIF-2α primary antibody with a dilution of 1:750 (Novus Biologicals) was added to each slide and allowed to sit overnight in 4 °C. Sections were incubated with horseradish peroxidase conjugated with anti-mouse IgG. Finally, slides were stained with DAB and counterstained with hematoxylin.

Statistical Analysis

Statistical significance was determined using a two-tailed unpaired Students t-test performed using Microsoft Office Excel 2010 (Microsoft, Redmond, WA, USA). $P \leq .05$ was considered significant unless otherwise stated.

Results

Validation of HIF Down-Regulation in Tumors with Immunohistochemistry

HIF-1α and HIF-2α down-regulation was confirmed by immunohistochemical analysis using the corresponding antibodies as shown in Figure 1, *A* and *B*. Because primary tumor growth was significantly delayed in 231-1α, 231-2α, and 231-DS tumors compared to 231-EV tumors, 231-EV tumors were excised at~ 300 to 450 mm^3 after approximately 10 weeks whereas 231-1α, 231-2α, and 231-DS tumors required approximately 23 to 27 weeks to attain comparable volumes.

Fiber Volumes Increase in 231-1α, 231-2α, and 231-DS Tumors

SHG microscopy was used to image Col1 fibers in tumors. Representative SHG images shown in Figure 2*A* illustrate differences in Col1 fibers in 231-1α, 231-2α and 231-DS tumors compared to EV tumors. An in-house fiber analysis software written in MATLAB was used to quantify fiber volume and fiber distance. Fiber volume in 231-1α, 231-2α and 231-DS tumors was significantly higher and inter-fiber distance was significantly lower compared to 231-EV tumors (Figure 2*B*).

Col1 fiber content was analyzed by COL1A1 immunostaining of tumor sections and immunoblotting of tumor tissue. Representative images of COL1A1 immunostained tumor sections are shown in Figure 3*A*. High-resolution digital scans of the immunostained sections were obtained using Aperio's Digital Pathology Slide Scanner (Leica Biosystems, Wetzlar, Germany). Images were processed and immunostaining intensity was quantified with Aperio ImageScope software using the algorithm supplied by the manufacturer (Leica Biosystems). Fractional COL1A1 immunostained areas were quantified by computing the fraction of strongly stained pixels in the tumor section normalized to the area of the section (1 section per

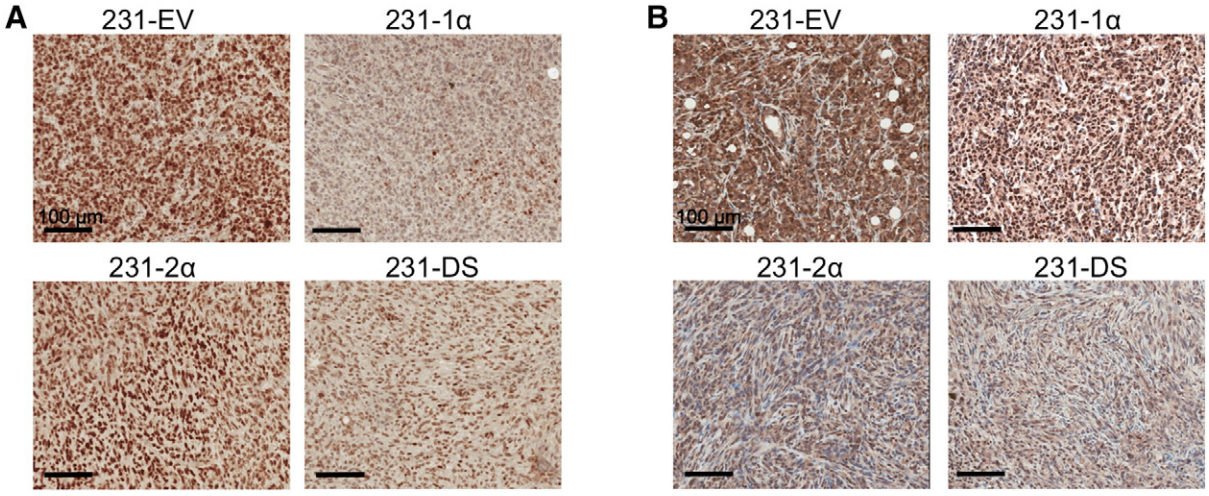

Figure 1. (A) Representative 20X images of HIF-1α immunostained sections demonstrating the reduction of HIF-1α in 231-1α and 231-DS tumors. (B) Representative 20× images of HIF-2α immunostained sections demonstrating the reduction of HIF-2α in 231-2α and 231-DS tumors.

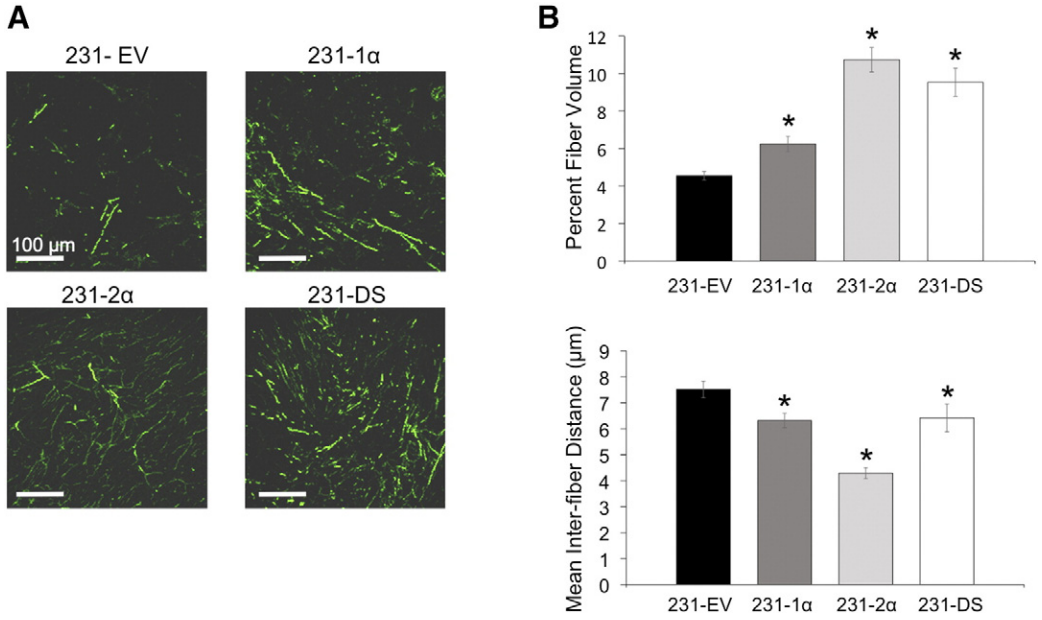

Figure 2. (A) Representative SHG microscopy images from viable tumor regions (field of view = 423.52 x 423.52 μm^2) showing increased Col1 fibers in tumors with HIF silencing. (B) Analysis from SHG microscopy showed that 231-1α ($P \leq .0005$), 231-2α ($P \leq .00005$), and 231-DS ($P \leq .00005$) contained significantly higher percent fiber volume compared to 231-EV tumors. There was no significant difference between the increase in fibers in 231-2α and the increase in 231-DS tumors. Distance between fibers was significantly reduced in 231-1α ($P \leq .05$), 231-2α ($P \leq .00005$) and 231-DS ($P \leq .05$) tumors compared to 231-EV. The reduction in 231-2α tumors was more drastic than in 231-1α and 231-DS tumors. Values represent mean ± S.E.M.

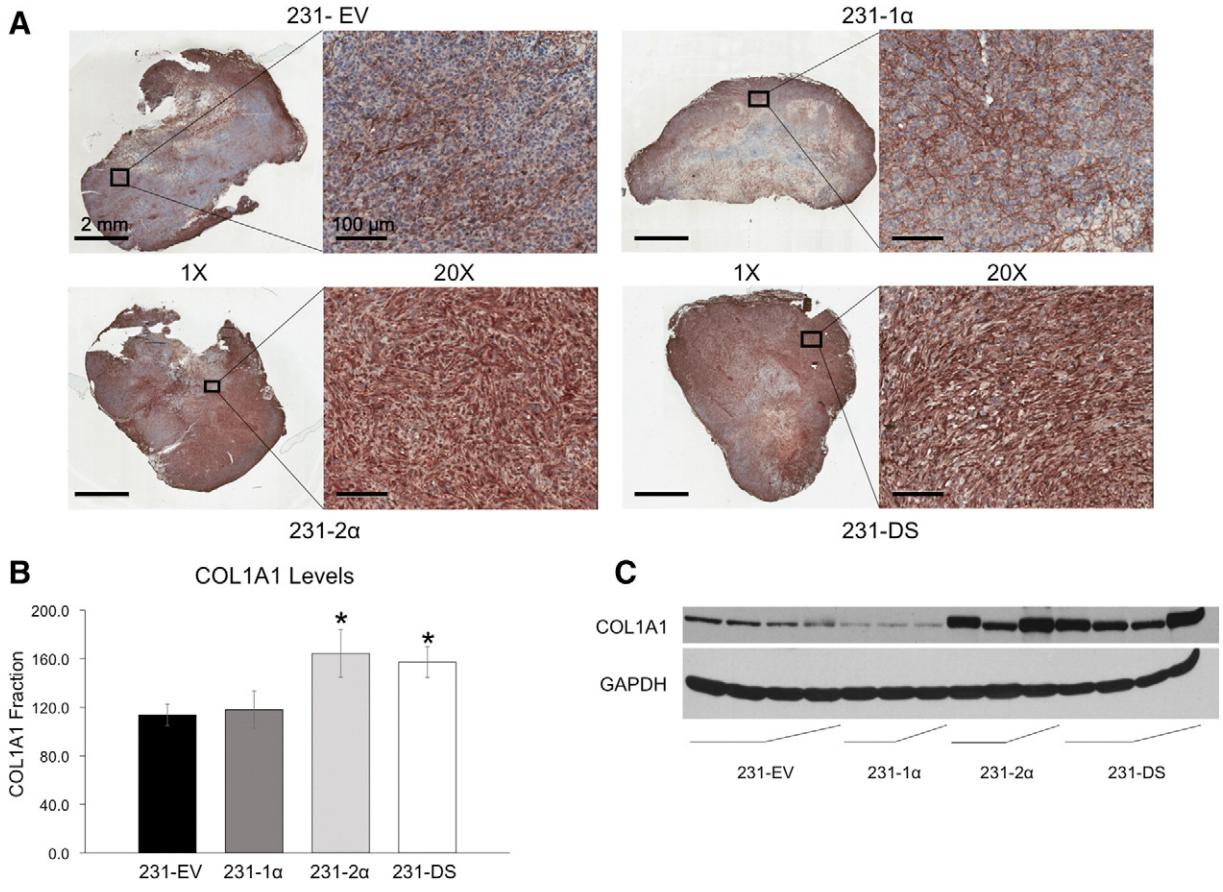

Figure 3. (A) Representative 1X and 20X images of COL1A1 immunostained tumor sections. (B) Quantification of strongly positive pixels normalized to the area of the tumor section. Values represent Mean ± S.E.M. * $P \leq .05$. (C) Representative immunoblots showing COL1A1 levels in 231-EV, 231-1α, 231-2α, and 231-DS tumors. GAPDH was used as a loading control.

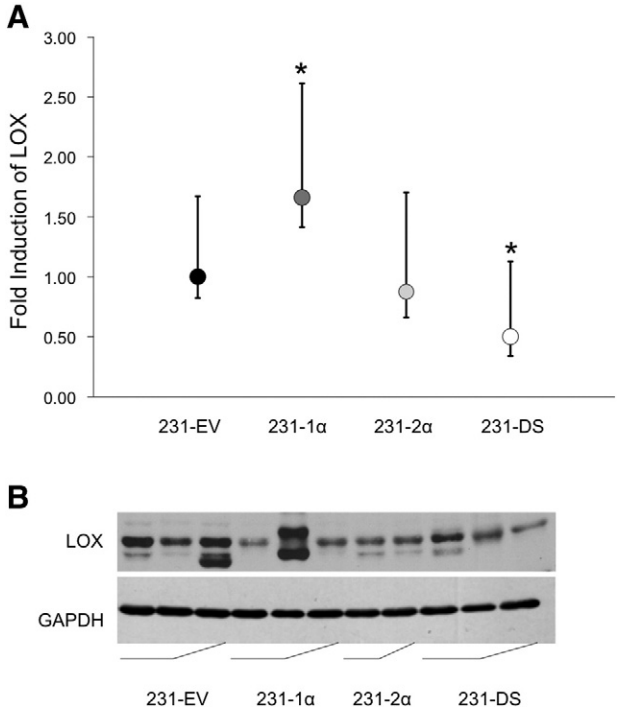

Figure 4. (A) LOX mRNA levels in 231-EV, 231-1α, 231-2α, and 231-DS tumors. Values represent mean, error bars represent the 95% confidence intervals. * $P \leq .05$. (B) Immunoblots of LOX protein expression in 231-EV, 231-1α, 231-2α, and 231-DS tumors. GAPDH was used as a loading control.

tumor). Strongly stained pixels were identified as strongly positive according to the Aperio software's Positive Pixel Count Algorithm. As shown in Figure 3*B*, the fractional COL1A1 immunostained area increased significantly in 231-2α and 231-DS tumors compared to 231-EV tumors ($P \leq .05$). Immunoblots of COL1A1 displayed in Figure 3*C* detected an increase of COL1A1 protein in 231-2α and 231-DS tumors.

Lysyl Oxidase Levels Were Reduced in 231-2α and 231-DS Tumors

Both mRNA levels and protein expression of LOX and LOX-L1 were quantified. A significant increase in LOX mRNA was observed in 231-1α tumors while a significant decrease was observed in 231-DS tumors (Figure 4*A*).

Western blot analysis revealed a reduction of LOX in all HIF silenced tumors compared to 231-EV tumors (Figure 4*B*). The different banding pattern of the second sample in the 231-1α group may have occurred from nonspecific binding or degradation of the protein. LOX-L1 immunoblot analysis showed no change in expression of LOX-L1 in HIF-silenced tumors compared to 231-EV (data not shown).

Matrix Metalloproteinases 1 and 14 Down-Regulated in 231-1α, 231-2α, and 231-DS Tumors

To determine whether MMP levels were altered in response to HIF silencing, qRT-PCR and immunoblotting were performed. The qRT-PCR results indicated that MMP-1 was reduced in 231-2α and 231-DS tumors and MMP-14 was reduced in all HIF-silenced tumors: 231-1α, 231-2α, and 231-DS (Figure 5, *A* and *B*). Western blot analyses detected a loss of expression of the active form of MMP-1 in 231-2α and 231-DS tumors. Additionally, a significant reduction of MMP-14 was observed in 231-1α and 231-DS tumors (Figure 5*C*).

Prolyl Hydroxylase Subunits

Two enzymes involved in post transcriptional modification of Col1, prolyl 4-hydroxylase-α1 (P4HA1) and prolyl 4-hydroxylase-α2 (P4HA2), were measured. P4HA1 significantly decreased in 231-1α and 231-2α tumors (Figure 6*A*). On the other hand, P4HA2 significantly increased in 231-2α and 231-DS tumors but decreased in 231-1α tumors (Figure 6*B*).

CAFs Detected by α-SMA Immunostaining

To understand the role of CAFs in the differences in Col1 fiber patters, α-SMA immunostaining of the tumors was performed. Representative images shown in Figure 7*A* demonstrate an increase of α-SMA immunostaining in 231-DS tumors. Quantitative estimates of α-SMA immunostained regions relative to tumor area revealed a significant increase of CAFs in 231-DS compared to 231-EV tumors as shown in Figure 7*B*.

Discussion

Col1 fiber content and patterns in tumors are the net outcome of several factors including enzymes such as LOX and P4Hs required for Col1 synthesis [17,18], MMPs that degrade Col1 fibers [27], and CAFs that are a primary source of Col1 [33,34]. Our purpose here was to understand the impact of HIF silencing on Col1 fiber content and on the molecular mechanisms that play a major role in the formation of Col1 fibers. The importance of HIFs in cancer progression has been well established [39]. Understanding the relationship between these parameters can provide further insight into the mechanisms by which these contribute to tumor progression and metastasis.

Tumors derived from HIF-1α, HIF-2α or combined HIF-1α and HIF-2α silenced MDA-MB-231 cells showed a significant increase of Col1 fiber volume and decrease of Col1 inter-fiber distance. This increase was more pronounced for HIF-2α and combined HIF-1α and HIF-2α silenced tumors. The decrease in inter-fiber distance was more drastic in 231-2α tumors than in 231-DS tumors perhaps suggesting a different rearrangement of fibers when only HIF-2α is down-regulated compared to when both HIF-1α and HIF-2α are down-regulated. We previously observed that hypoxic tumor regions contained fewer Col1 fibers [37], suggesting that increased HIF expression reduced Col1 fibers. Consistent with these studies, here we found that silencing HIFs increased Col1 fibers as detected by SHG microscopy. Col1A1 immunostaining also detected a significant increase of Col1 fiber content in 231-2α and 231-DS tumors confirming the SHG data for these tumors. Enzymes such as LOX, MMP-1, MMP-14 and P4Hs that regulate Col1 fibers were perturbed by HIF silencing. CAFs significantly increased in 231-DS tumors. A previous study reported a decrease in collagen with HIF-silencing in tumors orthotopically implanted together with matrigel [40]. However, the picrosirius stain used detected all fibrillar collagen, including types I, II, III, V, XI, XXIV, and XXVII [41]. We specifically studied Col1 fibers in tumors that were implanted without matrigel.

Several studies have identified Col1 fiber density and COL1A1 expression as associated with increased metastasis [13,15]. Similarly, an increase of CAFs has been associated with more aggressive cancers

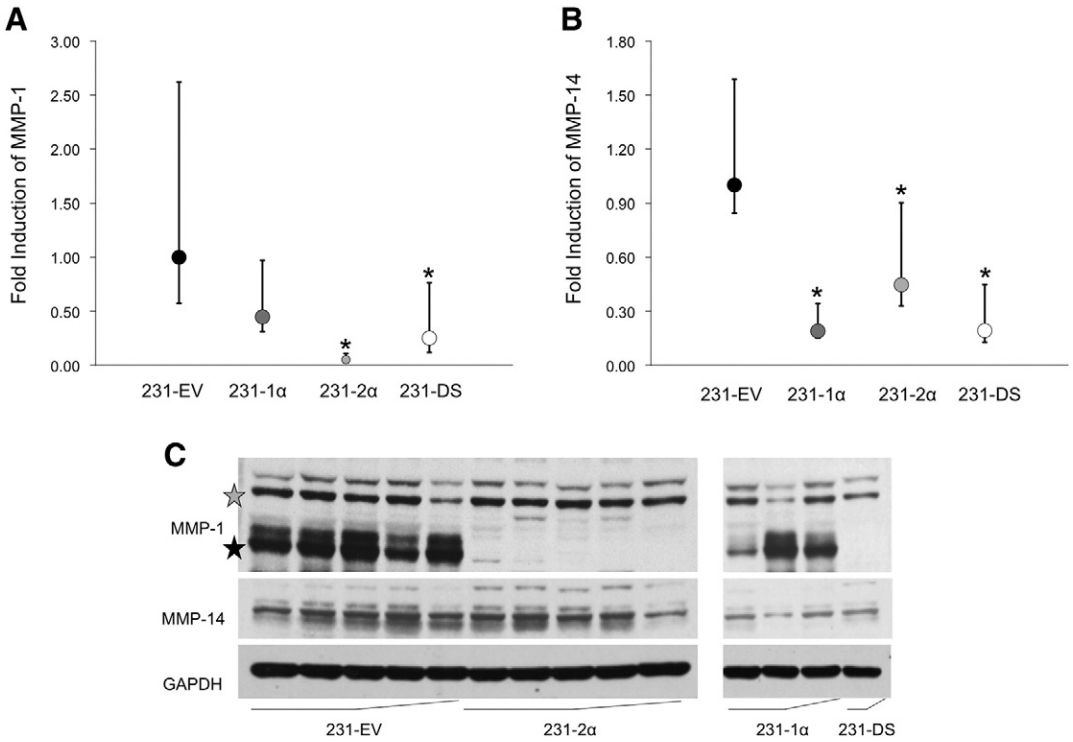

Figure 5. (A) MMP-1 and (B) MMP-14 mRNA expression in 231-EV, 231-1α, 231-2α, and 231-DS tumors. Values represent mean, error bars represent the 95% confidence interval. * $P \leq .05$. (C) Representative immunoblots from tumor samples showing MMP-1 and MMP-14 expression. GAPDH was used as a loading control. Gray star represents inactive MMP-1 and the black star represents active MMP-1.

[42–44]. In previous studies, we observed that HIF silencing reduced invasion and metastasis from MDA-MB-231 tumors [35]. Despite an increase of Col1 fibers in HIF silenced tumors observed here, the reduction of invasion may have reduced metastasis from these tumors [35]. These data highlight the importance of HIF regulated cytokines and pathways in the metastatic cascade and suggest that while Col1 fibers play a role in growth and metastasis [13–15], in the absence of these factors, cancer cells are limited in terms of growth and ability to metastasize. Cancer cells have been found to travel along radially aligned collagen fibers [13]. Alignment of fibers has been used to predict patient survival [45]. Another factor that may have contributed to the lack of metastasis despite the high Col1 is that fibers were not oriented to facilitate cancer cell migration. Knockdown of HIF-1α has been previously found to decrease alignment of fibers in tumors when exposed to hypoxia in comparison to EV tumors [40]. Col1 is a fibrillar collagen composed of repeating sequences of three amino acids in the form of GXY where X is typically a proline. Glycine and proline are the major amino acid precursors of Col1. Previous studies have identified regulation of glycine and proline by HIFs [46], suggesting that the metabolic

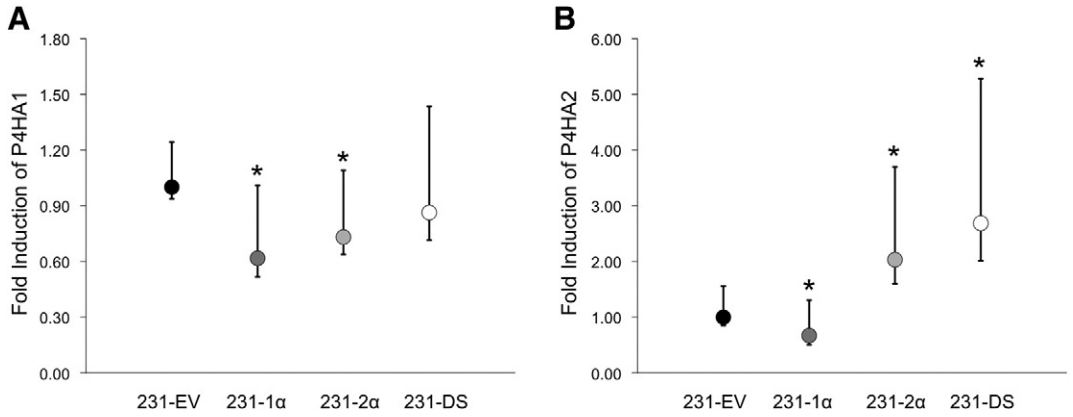

Figure 6. (A) P4HA1 and (B) P4HA2 mRNA expression in 231-EV, 231-1α, 231-2α, and 231-DS tumors. Values represent mean, error bars represent the 95% confidence intervals. * $P \leq .05$.

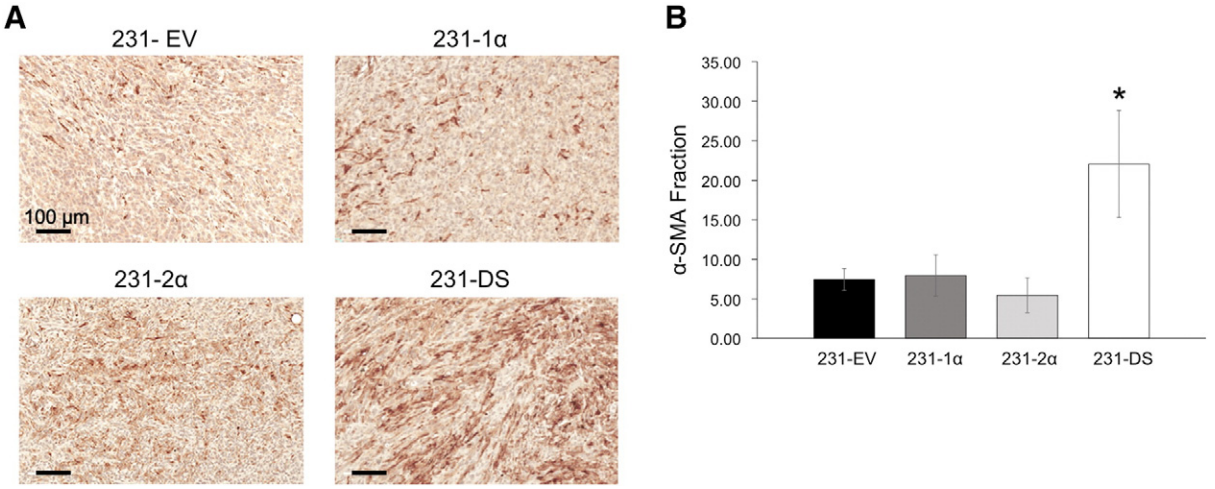

Figure 7. (A) Representative images of α-SMA immunostained tumor sections demonstrating an increase of CAFs in 231-DS tumors. (B) Quantification of strongly positive pixels normalized to the area of the tumor section. Values represent Mean ± S.E.M. * $P \leq .05$.

consequences of HIF silencing may have also played a role in the Col1 changes observed here and may have also reduced the ability of cells to invade and metastasize.

To understand mechanisms underlying the changes in Col1, we analyzed LOX responsible for cross-linking of Col1, MMPs involved in Col1 degradation, and P4Hs that perform post transcriptional modification of Col1 fibers. P4H consists of two subunits, α and β, which come together to form a tetramer. There are three isoforms of the α subunit, P4HA1, P4HA2, and P4HA3 [17]. Changes in the parameters investigated are summarized in Table 1. In 231-1α tumors, an increase of SHG detected Col1 fibers was accompanied by a reduction of MMP-14 mRNA and protein and a decrease of P4HA1 and P4HA2 mRNA. LOX mRNA increased but protein expression decreased in these tumors. COL1A1 immunostaining remained unchanged and COL1A1 protein decreased. It is possible that the COL1A1 antibody only recognized three-dimensional epitopes and had diminished reactivity with denatured Col1 fibers. CAFs did not increase in 231-1α tumors. In 231-2α tumors, an increase of SHG detected Col1 fibers was accompanied by an increase of COL1A1 immunostaining, COL1A1 protein, a decrease of LOX protein, a decrease of MMP-1 mRNA and protein, a decrease of MMP-14 mRNA, and a decrease of P4HA1 but an increase of P4HA2 mRNA. CAFs did not increase in these tumors. In 231-DS, the increase of SHG detected Col1 fibers was accompanied by an increase of COL1A1 immunostaining, COL1A1 protein, a decrease of LOX mRNA and protein, a decrease of MMP-1 and MMP-14 mRNA and protein, no change in P4HA1 and an increase of P4HA2 mRNA. CAFs significantly increased in 231-DS tumors.

Table 1. Summary of significant changes observed in the tumors. All comparisons are made with respect to 231-EV tumors

Parameters	231-1α	231-2α	231-DS
Col1 fiber percent volume	↑	↑	↑
Col1 fiber inter distance	↓	↓	↓
COL1A1 IHC	ns	↑	↑
COL1A1 protein	↓	↑	↑
LOX mRNA	↑	ns	↓
LOX protein	↓(2/3 tumors)	↓	↓
MMP1 mRNA	ns	↓	↓
MMP1 protein (inactive)	ns	ns	ns
MMP1 protein (active)	ns	↓	↓
MMP14 mRNA	↓	↓	↓
MMP14 protein	↓	ns	↓
P4HA1 mRNA	↓	↓	ns
P4HA2 mRNA	↓	↑	↑
CAFs (α-SMA IHC)	ns	ns	↑

The increase in Col1 fibers with HIF-1α, HIF-2α and HIF-1α and HIF-2α silencing may have been predominantly mediated through the reduction of MMPs as these were consistently lower in all three tumor types. MMP-1 and MMP-14 function to degrade Col1 fibers [27]. The reduction of MMP-1 and MMP-14 in HIF-silenced tumors indicates a reduction of Col1 degrading enzymes that is consistent with the increase of Col1 fibers observed with HIF silencing. MMPs are hypoxia regulated genes and thus reduced MMP expression in HIF silenced tumors alone is not surprising [47,48].

P4Hs are post transcriptional modifiers of Col1 required to form the triple helix of Col1 and promote its stabilization. The subunit P4HA1 is expressed mostly in mesenchymal cell types, while subunit P4HA2 is found mainly in differentiated cell types, chondrocytes, and osteoblasts [49]. Interestingly, the two subunits showed somewhat differing trends. P4HA1 was reduced in 231-1α and 231-2α. P4HA2, however, increased in 231-2α and 231-DS tumors, but decreased in 231-1α. An association between CO1A1 levels and P4HA2 has been previously reported [50]. In 231-DS tumors the only significant change was an increase in P4HA2. The increase of P4HA2 may explain, in part, the increase of Col1 fibers in 231-2α and 231-DS tumors.

LOX plays a key role in maintaining the stability of the ECM through its ability to catalyze the covalent cross-linking of Col1 fibers [19]. Both LOX and LOX-L1 are specifically associated with Col1 fibers [51]. For both 231-2α and 231-DS tumors, LOX protein expression was down-regulated compared to 231-EV tumors. LOX mRNA increased in 231-1α tumors although protein expression was reduced in two of three tumors. Taken together, the LOX results suggest that the amount of cross-linked fibers was overall reduced in the HIF-silenced tumors. Since non-cross-linked fibers also produce SHG signal [52], the increased Col1 fibers detected by SHG in HIF-silenced tumors may have been the result of partially processed

fibers. Cancer cell metastasis was found to be dependent upon LOX-mediated Col1 cross-linking [21,51]. Thus, the observed decrease in LOX could partly explain the lack of metastasis in the HIF-silenced tumors [35].

The increase of CAFs observed in 231-DS tumors may have contributed to the increase of Col1 fibers in these tumors, unlike the 231-1α and 231-2α tumors where we did not detect an increase of CAFs. The presence of CAFs is usually associated with increased aggressiveness [42–44] but our data suggest that without active HIF signaling, CAFs are rendered nonthreatening although they may still modify the ECM through increased Col1 deposition. Further studies are required to understand why HIF silencing increased the number of CAFs in these tumors.

In summary, HIF silencing increased tumor Col1 fiber density. The changes in Col1 fiber density were explained by a combination of changes in P4Hs, MMP-1, MMP-14, and LOX. The increased P4HA2 levels observed in 231-2α and 231-DS tumors likely up-regulated Col1 synthesis. The decrease in MMP-1 and MMP-14 levels in HIF-silenced tumors likely prevented Col1 degradation. The reduction of LOX protein expression suggests that there were fewer cross-linked fibers despite an overall increase in fiber density. CAFs contributed to the increase of Col1 fibers but only in 231-DS tumors. These data expand our understanding of HIF-mediated regulation of Col1 fibers in the TME and further highlight the importance of hypoxia in modifying the ECM.

Acknowledgments

Support from NIH R01CA73850, R01CA82237, R35CA209960, and P30CA006973 is gratefully acknowledged. We thank Mr. Gary Cromwell for valuable technical assistance.

References

[1] Gilkes DM and Semenza GL (2013). Role of hypoxia-inducible factors in breast cancer metastasis. *Future Oncol* **9**, 1623–1636.
[2] Gu YZ, Moran SM, Hogenesch JB, Wartman L, and Bradfield CA (1998). Molecular characterization and chromosomal localization of a third alpha-class hypoxia inducible factor subunit, HIF3alpha. *Gene Expr* **7**, 205–213.
[3] Hu CJ, Wang LY, Chodosh LA, Keith B, and Simon MC (2003). Differential roles of hypoxia-inducible factor 1alpha (HIF-1alpha) and HIF-2alpha in hypoxic gene regulation. *Mol Cell Biol* **23**, 9361–9374.
[4] Keith B, Johnson RS, and Simon MC (2011). HIF1alpha and HIF2alpha: sibling rivalry in hypoxic tumour growth and progression. *Nat Rev Cancer* **12**, 9–22.
[5] Dent R, Trudeau M, Pritchard KI, Hanna WM, Kahn HK, Sawka CA, Lickley LA, Rawlinson E, Sun P, and Narod SA (2007). Triple-negative breast cancer: clinical features and patterns of recurrence. *Clin Cancer Res* **13**, 4429–4434.
[6] Gangi A, Chung A, Mirocha J, Liou DZ, Leong T, and Giuliano AE (2014). Breast-conserving therapy for triple-negative breast cancer. *JAMA Surg* **149**, 252–258.
[7] Jin MS, Lee H, Park IA, Chung YR, Im SA, Lee KH, Moon HG, Han W, Kim K, and Kim TY, et al (2016). Overexpression of HIF1alpha and CAXI predicts poor outcome in early-stage triple negative breast cancer. *Virchows Arch* **469**, 183–190.
[8] Cecil DL, Slota M, O'Meara MM, Curtis BC, Gad E, Dang Y, Herendeen D, Rastetter L, and Disis ML (2017). Immunization against HIF-1alpha inhibits the growth of basal mammary tumors and targets mammary stem cells in vivo. *Clin Cancer Res* **23**, 3396–3404.
[9] Sahai E (2005). Mechanisms of cancer cell invasion. *Curr Opin Genet Dev* **15**, 87–96.
[10] Zhu J, Liang L, Jiao Y, Liu L, and Alliance US-CPS-O (2015). Enhanced invasion of metastatic cancer cells via extracellular matrix interface. *PLoS One* **10**, e0118058.
[11] Wirtz D, Konstantopoulos K, and Searson PC (2011). The physics of cancer: the role of physical interactions and mechanical forces in metastasis. *Nat Rev Cancer* **11**, 512–522.
[12] Gilkes DM, Bajpai S, Chaturvedi P, Wirtz D, and Semenza GL (2013). Hypoxia-inducible factor 1 (HIF-1) promotes extracellular matrix remodeling under hypoxic conditions by inducing P4HA1, P4HA2, and PLOD2 expression in fibroblasts. *J Biol Chem* **288**, 10819–10829.
[13] Provenzano PP, Eliceiri KW, Campbell JM, Inman DR, White JG, and Keely PJ (2006). Collagen reorganization at the tumor-stromal interface facilitates local invasion. *BMC Med* **4**, 38.
[14] Provenzano PP, Inman DR, Eliceiri KW, Knittel JG, Yan L, Rueden CT, White JG, and Keely PJ (2008). Collagen density promotes mammary tumor initiation and progression. *BMC Med* **6**, 11.
[15] Kakkad SM, Solaiyappan M, Argani P, Sukumar S, Jacobs LK, Leibfritz D, Bhujwalla ZM, and Glunde K (2012). Collagen I fiber density increases in lymph node positive breast cancers: pilot study. *J Biomed Opt* **17**, 116017.
[16] Malfait F, Symoens S, Coucke P, Nunes L, De Almeida S, and De Paepe A (2006). Total absence of the alpha2(I) chain of collagen type I causes a rare form of Ehlers-Danlos syndrome with hypermobility and propensity to cardiac valvular problems. *J Med Genet* **43**e36.
[17] Gorres KL and Raines RT (2010). Prolyl 4-hydroxylase. *Crit Rev Biochem Mol Biol* **45**, 106–124.
[18] Siegel RC, Pinnell SR, and Martin GR (1970). Cross-linking of collagen and elastin. Properties of lysyl oxidase. *Biochemistry* **9**, 4486–4492.
[19] Smith-Mungo LI and Kagan HM (1998). Lysyl oxidase: properties, regulation and multiple functions in biology. *Matrix Biol* **16**, 387–398.
[20] Helleman J, Jansen MP, Ruigrok-Ritstier K, van Staveren IL, Look MP, Meijer-van Gelder ME, Sieuwerts AM, Klijn JG, Sleijfer S, and Foekens JA, et al (2008). Association of an extracellular matrix gene cluster with breast cancer prognosis and endocrine therapy response. *Clin Cancer Res* **14**, 5555–5564.
[21] Erler JT, Bennewith KL, Nicolau M, Dornhofer N, Kong C, Le QT, Chi JT, Jeffrey SS, and Giaccia AJ (2006). Lysyl oxidase is essential for hypoxia-induced metastasis. *Nature* **440**, 1222–1226.
[22] Barker HE, Chang J, Cox TR, Lang G, Bird D, Nicolau M, Evans HR, Gartland A, and Erler JT (2011). LOXL2-mediated matrix remodeling in metastasis and mammary gland involution. *Cancer Res* **71**, 1561–1572.
[23] Peinado H, Moreno-Bueno G, Hardisson D, Perez-Gomez E, Santos V, Mendiola M, de Diego JI, Nistal M, Quintanilla M, and Portillo F, et al (2008). Lysyl oxidase-like 2 as a new poor prognosis marker of squamous cell carcinomas. *Cancer Res* **68**, 4541–4550.
[24] Kirschmann DA, Seftor EA, Fong SF, Nieva DR, Sullivan CM, Edwards EM, Sommer P, Csiszar K, and Hendrix MJ (2002). A molecular role for lysyl oxidase in breast cancer invasion. *Cancer Res* **62**, 4478–4483.
[25] Wong CC, Gilkes DM, Zhang H, Chen J, Wei H, Chaturvedi P, Fraley SI, Wong CM, Khoo US, and Ng IO, et al (2011). Hypoxia-inducible factor 1 is a master regulator of breast cancer metastatic niche formation. *Proc Natl Acad Sci U S A* **108**, 16369–16374.
[26] Wang V, Davis DA, and Yarchoan R (2017). Identification of functional hypoxia inducible factor response elements in the human lysyl oxidase gene promoter. *Biochem Biophys Res Commun* **490**, 480–485.
[27] Fields GB (2013). Interstitial collagen catabolism. *J Biol Chem* **288**, 8785–8793.
[28] Liu H, Kato Y, Erzinger SA, Kiriakova GM, Qian Y, Palmieri D, Steeg PS, and Price JE (2012). The role of MMP-1 in breast cancer growth and metastasis to the brain in a xenograft model. *BMC Cancer* **12**, 583.
[29] Sato H, Takino T, Okada Y, Cao J, Shinagawa A, Yamamoto E, and Seiki M (1994). A matrix metalloproteinase expressed on the surface of invasive tumour cells. *Nature* **370**, 61–65.
[30] Itoh Y (2015). Membrane-type matrix metalloproteinases: Their functions and regulations. *Matrix Biol* **44-46**, 207–223.
[31] Sabeh F, Ota I, Holmbeck K, Birkedal-Hansen H, Soloway P, Balbin M, Lopez-Otin C, Shapiro S, Inada M, and Krane S, et al (2004). Tumor cell traffic through the extracellular matrix is controlled by the membrane-anchored collagenase MT1-MMP. *J Cell Biol* **167**, 769–781.
[32] Sato H and Seiki M (1996). Membrane-type matrix metalloproteinases (MT-MMPs) in tumor metastasis. *J Biochem* **119**, 209–215.
[33] Kalluri R and Zeisberg M (2006). Fibroblasts in cancer. *Nat Rev Cancer* **6**, 392–401.
[34] Kalluri R (2016). The biology and function of fibroblasts in cancer. *Nat Rev Cancer* **16**, 582–598.

[35] Shah T, Krishnamachary B, Wildes F, Mironchik Y, Kakkad SM, Jacob D, Artemov D, and Bhujwalla ZM (2015). HIF isoforms have divergent effects on invasion, metastasis, metabolism and formation of lipid droplets. *Oncotarget* **6**, 28104–28119.

[36] Krishnamachary B, Penet M-F, Nimmagadda S, Mironchik Y, Raman V, Solaiyappan M, Semenza GL, Pomper MG, and Bhujwalla ZM (2012). Hypoxia Regulates CD44 and Its Variant Isoforms through HIF-1α in Triple Negative Breast Cancer. *PLoS One* **7**e44078.

[37] Kakkad SM, Solaiyappan M, O'Rourke B, Stasinopoulos I, Ackerstaff E, Raman V, Bhujwalla ZM, and Glunde K (2010). Hypoxic tumor microenvironments reduce collagen I fiber density. *Neoplasia* **12**, 608–617.

[38] Fu WJ, Hu J, Spencer T, Carroll R, and Wu G (2006). Statistical models in assessing fold change of gene expression in real-time RT-PCR experiments. *Comput Biol Chem* **30**, 21–26.

[39] Semenza GL (2012). Hypoxia-inducible factors: mediators of cancer progression and targets for cancer therapy. *Trends Pharmacol Sci* **33**, 207–214.

[40] Gilkes DM, Chaturvedi P, Bajpai S, Wong CC, Wei H, Pitcairn S, Hubbi ME, Wirtz D, and Semenza GL (2013). Collagen prolyl hydroxylases are essential for breast cancer metastasis. *Cancer Res* **73**, 3285–3296.

[41] Pierard GE (1989). Sirius red polarization method is useful to visualize the organization of connective tissues but not the molecular composition of their fibrous polymers. *Matrix* **9**, 68–71.

[42] Krishnamachary B, Stasinopoulos I, Kakkad S, Penet MF, Jacob D, Wildes F, Mironchik Y, Pathak AP, Solaiyappan M, and Bhujwalla ZM (2017). Breast cancer cell cyclooxygenase-2 expression alters extracellular matrix structure and function and numbers of cancer associated fibroblasts. *Oncotarget* **8**, 17981–17994.

[43] Mao Y, Keller ET, Garfield DH, Shen K, and Wang J (2013). Stromal cells in tumor microenvironment and breast cancer. *Cancer Metastasis Rev* **32**, 303–315.

[44] Orimo A, Gupta PB, Sgroi DC, Arenzana-Seisdedos F, Delaunay T, Naeem R, Carey VJ, Richardson AL, and Weinberg RA (2005). Stromal fibroblasts present in invasive human breast carcinomas promote tumor growth and angiogenesis through elevated SDF-1/CXCL12 secretion. *Cell* **121**, 335–348.

[45] Conklin MW, Eickhoff JC, Riching KM, Pehlke CA, Eliceiri KW, Provenzano PP, Friedl A, and Keely PJ (2011). Aligned collagen is a prognostic signature for survival in human breast carcinoma. *Am J Pathol* **178**, 1221–1232.

[46] Cuperlovic-Culf M, Cormier K, Touaibia M, Reyjal J, Robichaud S, Belbraouet M, and Turcotte S (2016). (1)H NMR metabolomics analysis of renal cell carcinoma cells: Effect of VHL inactivation on metabolism. *Int J Cancer* **138**, 2439–2449.

[47] Miyoshi A, Kitajima Y, Ide T, Ohtaka K, Nagasawa H, Uto Y, Hori H, and Miyazaki K (2006). Hypoxia accelerates cancer invasion of hepatoma cells by upregulating MMP expression in an HIF-1alpha-independent manner. *Int J Oncol* **29**, 1533–1539.

[48] Fu OY, Hou MF, Yang SF, Huang SC, and Lee WY (2009). Cobalt chloride-induced hypoxia modulates the invasive potential and matrix metalloproteinases of primary and metastatic breast cancer cells. *Anticancer Res* **29**, 3131–3138.

[49] Nissi R, Autio-Harmainen H, Marttila P, Sormunen R, and Kivirikko KI (2001). Prolyl 4-hydroxylase isoenzymes I and II have different expression patterns in several human tissues. *J Histochem Cytochem* **49**, 1143–1153.

[50] Xiong G, Deng L, Zhu J, Rychahou PG, and Xu R (2014). Prolyl-4-hydroxylase alpha subunit 2 promotes breast cancer progression and metastasis by regulating collagen deposition. *BMC Cancer* **14**, 1.

[51] Cox TR, Bird D, Baker AM, Barker HE, Ho MW, Lang G, and Erler JT (2013). LOX-mediated collagen crosslinking is responsible for fibrosis-enhanced metastasis. *Cancer Res* **73**, 1721–1732.

[52] Lutz V, Sattler M, Gallinat S, Wenck H, Poertner R, and Fischer F (2012). Impact of collagen crosslinking on the second harmonic generation signal and the fluorescence lifetime of collagen autofluorescence. *Skin Res Technol* **18**, 168–179.